Study of resolution limits due to intrinsic bias in chemically amplified photoresists

Sergei V. Postnikov[a)]
Department of Chemistry, The University of Texas at Austin, Austin, Texas 78712

Michael D. Stewart
Department of Chemical Engineering, The University of Texas at Austin, Austin, Texas 78712

Hoang Vi Tran
Department of Chemistry, The University of Texas at Austin, Austin, Texas 78712

Mark A. Nierode
Department of Chemical Engineering, The University of Texas at Austin, Austin, Texas 78712

David R. Medeiros and T. Cao
Department of Chemistry, The University of Texas at Austin, Austin, Texas 78712

Jeffrey Byers
International SEMATECH, 2706 Montopolis Drive, Austin, Texas 78741

Stephen E. Webber and C. Grant Wilson
Department of Chemistry, The University of Texas at Austin, Austin, Texas 78712

(Received 4 June 1999; accepted 17 September 1999)

This article presents experimental results that suggest that classical Fickian diffusion cannot account for any significant fraction of the critical dimension bias observed in chemically amplified photoresists. A transport mechanism based on reaction front propagation is proposed as a possible explanation for the experimental observations. © *1999 American Vacuum Society.* [S0734-211X(99)18206-4]

I. INTRODUCTION

Critical dimension (CD) bias, linewidth spread, and isofocal bias are terms well known to those who use chemically amplified photoresists (CARs) in microlithography. These terms describe the image blur that has typically been attributed to Fickian diffusion of the acid catalyst from exposed regions into unexposed regions.[1,2] Photoresist formulations use base additives and photoacid generators (PAGs) that produce acids with bulky conjugate bases to minimize this spread, but there is always some bias at the optimum process condition. Bias refers to the difference between a feature's targeted dimension and the actual feature dimension printed in the photoresist. The objective of this work was to directly quantify the contribution of catalyst migration to CD bias and to establish a better understanding of the transport phenomena responsible for catalyst migration.

Previous studies of acid transport in CARs have used lithographic processes to infer acid diffusion coefficients.[1,3] The drawback to this approach is that individual contributions to bias are difficult to deconvolve and little insight into the actual transport phenomena responsible for migration is gained. Several experimental techniques were designed and tested in an attempt to directly measure acid diffusion coefficients in polymers. Experimental techniques based on capacitance measurements, diffraction grating analysis, and atomic force microscopy were utilized to monitor acid migration in resist polymers. Despite the documented sensitivity of these experimental techniques, when the analyzed material was poly(4-hydroxystyrene) (PHS), a major component of CARs, no diffusive transport could be documented at typical resist processing temperatures. A new technique for measuring acid transport based on Fourier transform infrared (FT-IR) spectroscopy was devised.[4] This approach requires creation of a trilayer ''sandwich'' of polymer films.

The sandwich technique has been used by others to study diffusion of various penetrants in thin polymer films. For example, Torkelson *et al.* used the sandwich structure and fluorescence nonradiative energy transfer to measure diffusion of small dye molecules in various polymer films.[5] Lin *et al.* used the sandwich technique and neutron reflectometry for measuring interdiffusion of isotopically labeled poly(methyl methacrylate) and unlabeled poly(methyl methacrylate).[6]

The first sandwich layer is a polymer containing a photoacid generator, which upon ultraviolet (UV) exposure serves as the acid reservoir. An intermediate polymer layer was placed on the reservoir layer. Finally, an acid detector layer of poly(*t*-butyloxycarbonyloxystyrene) (*t*-BOC) was placed on top of the intermediate layer. This created a trilayer stack in which the acid layer was separated from *t*-BOC by an intermediate polymer layer of known thickness. Acid generated in the reservoir layer by UV exposure would be expected to diffuse through the intermediate layer, then subsequently penetrate into the detector layer. When acid arrives at the detector layer, *t*-BOC is quickly converted into PHS. This conversion is easily measured during the course of the experiment by monitoring the absorbance of the carbonate carbonyl in the infrared.

[a)] Electronic mail: sergei@mail.utexas.edu

II. EXPERIMENT

A. Materials

The *t*-BOC used as detector layer in this study was prepared by free radical polymerization of *t*-butyloxycarbonyloxystyrene monomer from Hoechst Chemical Co. Poly(ethyl methacrylate) (PEMA) and PHS were used as intermediate layers in this study. PEMA was obtained from Dupont and used as received. PHS was synthesized in our laboratory according to reported procedures[7] from *p*-acetoxystyrene monomer supplied by Triquest. Poly(4-methoxystyrene) was synthesized from PHS, methyl iodide, and base. The photoacid generators bis(*p*-tert-butylphenyl)iodonium trifluoromethanesulfonate (PAG No. 1) and bis(*p*-tert-butylphenyl)iodonium perfluorobutanesulfonate (PAG No. 2) were provided by Midori Kagaku, Co. Triphenylsulfonium perfluorobutanesulfonate (PAG No. 3) was synthesized in our lab according to reported procedures.[8] The casting solvent for PHS was ethanol. The casting solvent for *t*-BOC was either toluene or propylene glycol methyl ether acetate (PGMEA) depending on the sample preparation method employed. All other polymers were cast from PGMEA. Solvents were purchased from Aldrich Chemical Co. and used as received.

B. Apparatus

A Nicolet Magna 550 FT-IR with a liquid nitrogen cooled MCT/B external IR detector from Axiom Analytical was used to collect sample spectra. A nitrogen purged sample chamber attached to a temperature controlled hotplate allowed sample spectra to be collected at elevated temperatures. The samples were exposed with a JBA high performance collimated UV light source through an Acton Research Corp. 248 nm interference filter.

C. Sample preparation

Samples were prepared on double-polished silicon substrates coated with gold on one side. The gold coating allowed IR measurements to be made in reflection mode. When casting solvents could be matched such that each layer was insoluble in the casting solvent for the subsequent layer, trilayer stacks necessary for these experiments were made directly by sequential spin casting. Often this requirement could not be met and an alternative, film float approach was employed. This float method required spin casting each layer on separate glass substrates, then floating the polymer films onto the surface of water from the glass substrates. The floating films were then picked up on the sample substrate bearing the underlying film layer(s). The samples were then dried by heating and/or vacuum desiccation. This method is, of course, limited to polymers that release from the substrate and maintain film integrity during floating. A series of control experiments were conducted to insure that the float process did not leach a significant amount of PAG out of the films or cross contaminate the layers.

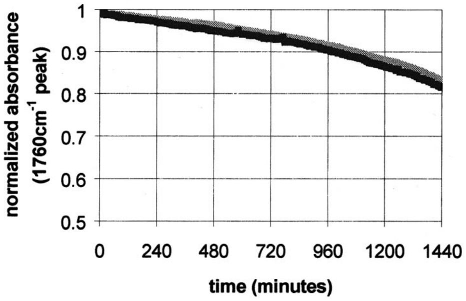

FIG. 1. PHS trilayer experiment at 90 °C. PHS layer 600 nm thick. (Gray line) sample with acid in the reservoir layer. PAG #1 (10 wt %) Dose: 60 mJ/cm^2. (Black line) sample with no PAG in reservoir layer.

III. RESULTS

Acid diffusion through PHS was never detected by the capacitance technique, the diffraction grating technique, or the atomic force microscopy technique.[4] These experiments were conducted at temperatures ranging from 25 to 150 °C. The diffusion coefficient inferred from these experiments is of magnitude of less than 10^{-8} μm^2/s. Spectroscopic techniques also never detected diffusion through PHS in any reasonable time. Figure 1 shows the detector layer response of a trilayer IR experiment using PHS as the intermediate layer. The experiment was conducted over a full day at 90 °C. There is clearly some detector layer response, but this response is the same as that of a control experiment in which no PAG was present in the feeder layer. The slope observed in Fig. 1 is thus not attributable to acid arrival, but is only the background, uncatalyzed thermolysis rate of *t*-BOC at 90 °C. These data indicate that the diffusion coefficient for this particular photoacid at 90 °C in PHS must then be less than 10^{-8} μm^2/s. Several different attempts were made to use this trilayer method to determine diffusion coefficients in PHS using very thin films and very long times, but acid arrival was never detected. If only Fickian diffusion is used to explain linewidth spread, the diffusion coefficients suggested by these experiments are far too small to account for the CD bias observed in actual manufacturing processes.

Experiments with other polymers besides PHS as the intermediate layer provide insight into the PHS observations. Several trilayer experiments using PEMA as the intermediate layer were carried out. This polymer has a lower glass transition temperature than PHS. Figure 2 shows the detector response curve for a trilayer PEMA experiment conducted at

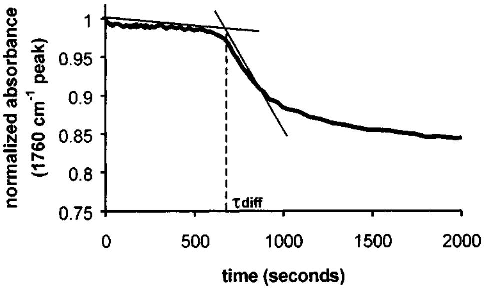

FIG. 2. Detector layer response curve for acid generated from PAG #2 showing diffusion through 435 nm PEMA layer at 90 °C. The diffusion time equals 615 s.

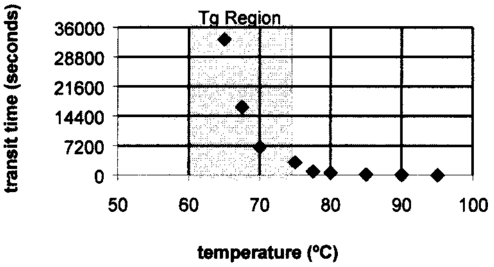

FIG. 3. Temperature dependence of acid diffusion through a 150 nm thick PEMA layer. PAG #2 (5 wt %) in reservoir layer. Dose: 60 mJ/cm^2.

90 °C. An induction period and arrival of acid at the detector layer are clearly seen in Fig. 2. A series of PEMA experiments was conducted with different intermediate layer thicknesses. Acid transit time was found to scale linearly with the square of PEMA layer thickness, as would be expected for classical Fickian diffusion. The diffusion coefficient obtained from this method is of the magnitude 10^{-4} μm^2/s. In another set of experiments the PEMA film thickness and the other parameters of the experiment were held constant and temperature was varied from 95 to 60 °C. As shown in Fig. 3, the acid transit time has a strong dependence on the bake temperature. The shaded box drawn in Fig. 3 spans the onset and completion temperatures of the glass transition as measured by differential scanning calorimetry. PEMA has a midpoint glass transition temperature T_g of approximately 68 °C. The T_g of PHS by comparison is approximately 180 °C. This difference in T_g explains why diffusion through PEMA at 90 °C is measurable while diffusion through PHS is not.

Since acid was not traversing the PHS intermediate layer at temperatures used in lithography applications, the detector layer was placed in direct contact with the acid reservoir layer. In these bilayer experiments, *t*-BOC served as both the detector layer and the analyzed intermediate layer. Somewhat surprising results were observed in these bilayer experiments. There was a fast initial apparent diffusion rate that slowed to a negligible rate after about 2.5 min. Figure 4 shows the results from a series of bilayer experiments run at four different temperatures. As expected, acid transport is dependent on the postexposure bake temperature. The slope of the curves after the fast reaction periods can be attributed mainly to background thermolysis. Concentration gradient driven diffusion cannot really explain this behavior.

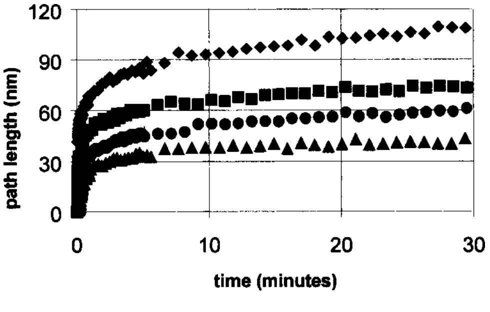

FIG. 4. Temperature dependence of acid path length in *t*-BOC. PAG #3 (10 wt %) in reservoir layer. 75 °C (▲), 90 °C (●), 100 °C (■), 110 °C (◆).

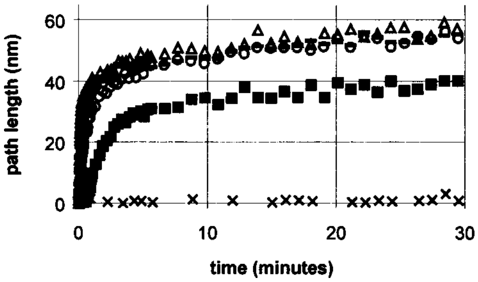

FIG. 5. Dependent of path length on reservoir layer acid concentration using PAG #2. Dose levels: 0.7 mJ/cm^2 (×), 3.5 mJ/cm^2 (■), 7.0 mJ/cm^2 (○), 13 mJ/cm^2 (—), 27 mJ/cm^2 (△).

Another series of bilayer experiments was conducted with various acid concentrations in the reservoir layer to determine the concentration dependence of transport path length. Figure 5 shows that there is a threshold level of concentration above which increasing the concentration has little effect on the path length. This result is another strong argument against Fickian transport, which predicts a concentration dependence.

Different concentrations of acid in the feeder layer were produced by varying the ultraviolet exposure dose. To ensure that the different doses actually created different concentrations, another set of experiments was necessary. PAG No. 2 (5 wt %) was added directly to a *t*-BOC solution. Films cast from this solution were then exposed to doses ranging from 0 to 90 mJ/cm^2, and the rate of deprotection was monitored by IR. The rate of the reaction increased steadily with increasing dose up to slightly greater than 30 mJ/cm^2. Thus, varying exposure doses from 0 to 30 mJ/cm^2 definitely results in progressively increasing acid concentration.

Attempts to explain the experimental data depicted in Figs. 4 and 5 from the standpoint of conventional diffusional formalism requires the diffusion rate to be very rapid for the first few minutes, then to drastically slow down. If the data were truncated at about 90 s (a typical PEB time), then the estimated diffusion coefficient to account for the observed movement would be about 10^{-4} μm^2/s which is the same order of magnitude reported previously from lithographic studies.[1]

If the results of the bilayer experiments are examined carefully, an apparent contradiction with the trilayer experiment is observed. As the acid propagates from the feeder layer into the *t*-BOC layer, it carries out a deprotection reaction which forms a layer of PHS between the source and the remaining detector layer. After a few seconds of reaction, the PHS barrier of the trilayer experiment has been recreated. We know that this PHS barrier prevents acid from the reservoir from reaching the detector layer. Thus, only the acid initial present at the interface is available to catalyze the reaction in the *t*-BOC bilayer experiments.

IV. DISCUSSION

Much previous work has shown that diffusivity in polymers is highly dependent on the sample temperature relative to the polymer's T_g. The diffusion of a variety of penetrants

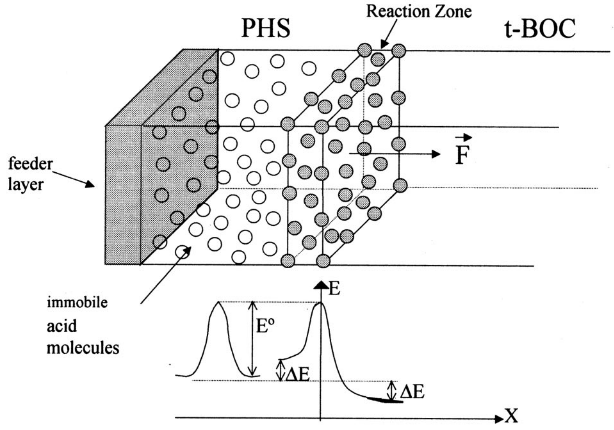

FIG. 6. Pictorial illustration of the reaction front propagation hypothesis. Solid circles represent active acid molecules in the front region. The empty circles represent immobilized acid molecules behind the front.

through polymers has been studied by other authors and the crucial effect of the glass transition temperature on diffusion rate has been well documented.[9–11] The free volume fraction is roughly the same in all polymers at the glass transition temperature,[12] so if the diffusion coefficient of a penetrant is known in a polymer at its T_g, it is possible to estimate the diffusivity of the same penetrant in a different polymer matrix by using the Williams–Landel–Ferry (WLF) equation.[13] The estimated diffusion coefficient for a polymer 20 °C below T_g turns out to be extremely low ($\sim 2\times 10^{-11}$ μm^2/s). This observation explains why diffusion in PHS at 100 °C was not measurable: at 100 °C, PHS is 80 °C below its T_g. The measured T_g of *t*-BOC is 125 °C,[4] yet Fig. 4 shows acid transport in *t*-BOC at temperatures well below T_g. If the WLF estimates for the diffusion coefficient in *t*-BOC are correct, Fickian diffusion certainly cannot explain the observed transport distances. Obviously, some other forces are in effect that aid acid transport in *t*-BOC. The most obvious difference between *t*-BOC and PHS is that the former reacts with acid and the latter does not. Therefore, a physical model that can explain the acid transport in *t*-BOC is a reaction front propagation mechanism. Figure 6 schematically depicts a reaction zone (front) at some time after it has advanced some distance into the *t*-BOC layer. The front can be thought of as an interface of finite volume between PHS and unreacted *t*-BOC. An attempt to explain this front propagation mechanism mathematically has been made by Neureuther *et al.*[15] The conversion of *t*-BOC into PHS is in progress within the frontal zone. The acid catalyst operates int his layer and is regenerated upon completion of the deprotection reaction. This zone thus becomes a secondary source of acid capable of initiating the reaction in the next finite zone of *t*-BOC. Thus, the reaction front propagates stepwise, layer by layer.

Acid molecules in the front (*t*-BOC/PHS interface) are located in an asymmetric physico-chemical environment. This asymmetry is created by virtue of the different affinity of the acid for the PHS hydroxyl group and *t*-BOC carbonyl group, possibly due to their different basicities. The *p*Ka's of protonated phenols and esters are approximately the same in aqueous media, but can be very different in the dry polymer film. Support for greater basicity of *t*-BOC compared with that of PHS is found in the work of Wallraff *et al.* who showed that the equilibrium between protonated phenol and protonated *t*-BOC had to be included in their kinetic model in order to fit experimental data.[14] Thus, it is reasonable to propose a slightly higher concentration of protonated species on the *t*-BOC side of the front than on the PHS side, resulting in a local electrical field across the field. This local field aids movement of bulky acid anion through the glassy polymer. Alternatively, excess free volume may be available for a short time in the reaction zone due to evolution of the gaseous species generated by the reaction.[15] There is a net flux of acid in the direction of *t*-BOC side stemming from some affinity differential. The preference for acid molecules to go into the *t*-BOC layer is of a statistical nature. Most move forward, driven by the affinity differential. Some percentage then jump back towards the PHS side. Molecules that jump backward become immobilized and no longer participate in the front propagation because the diffusion coefficient in PHS is extremely low. The acid trapped in PHS can be considered kinetically lost and unavailable to the front. If only a small percentage of acid jumps backward into PHS the concentration of acid in the front undergoes geometrical depletion in each step of propagation. This provides an explanation for the self-limiting nature of acid transport in *t*-BOC and explains why the front does not propagate infinitely.

ACKNOWLEDGMENTS

The authors would like to express appreciation to SRC (Contract No. 98-LC-460) and International SEMATECH for support. They would like to thank Midori Kagaku Co. and Kyle Patterson for providing the PAGs used in this work.

[1] T. Fedenyshyn, J. Thackeray, J. Georger, and M. Denison, J. Vac. Sci. Technol. B **12**, 3888 (1994).
[2] L. Schlegel, T. Ueno, N. Hayashi, and T. Iwayanagi, Jpn. J. Appl. Phys., Part 1 **11**, 30 (1991).
[3] J. Sturtevant, S. Holmes, and P. Rabidoux, Proc. SPIE **1672**, 114 (1992).
[4] S. Postnikov, Ph.D. Dissertation, The University of Texas at Austin, 1999.
[5] D. Hall and J. Torkelson, Macromolecules **31**, 8817 (1998).
[6] E. Lin, W. Wu, and S. Satija, Macromolecules **30**, 7224 (1997).
[7] J. Frechet, E. Eichler, H. Ito, and C. G. Willson, Polymer **24**, 995 (1983).
[8] J. Byers, K. Patterson, S. Cho, M. McCallum, and C. G. Willson, Photopolymer Sci. Technol. **11**, 465 (1998).
[9] J. S. Vrentas, H. T. Liu, and M. K. Lau, J. Appl. Polym. Sci. **27**, 3987 (1982).
[10] W. J. Koros and M. W. Hellums, ''Transport Properties'' in *Encyclopedia of Polymer Science and Engineering*, Supplement Volume, 2nd ed. (1989).
[11] G. J. Van Amergedon, Rubber Chem. Technol. **24**, 109 (1951).
[12] P. Munk, *Introduction to Macromolecular Science* (Wiley, New York, 1989).
[13] M. L. Williams, R. F. Landel, and J. D. Ferry, J. Am. Chem. Soc. **77**, 3701 (1955).
[14] G. M. Wallraff, W. D. Hinsberg, F. Houle, J. Optiz, and D. Hopper, Proc. SPIE **2438**, 182 (1995).
[15] E. Croffie, M. Cheng, and A. Neureuther, J. Vac. Sci. Technol. B (submitted).